Influence of the boundary conditions on the current flow pattern along a superconducting wire

Jorge Berger*
Department of Physics and Optical Engineering, Ort Braude College, 21982 Karmiel, Israel
(Received 30 January 2015; revised manuscript received 24 May 2015; published 17 August 2015)

We study the patterns at which the current flow stabilizes in a finite 1D superconducting wire, for various experimentally reasonable boundary conditions, for small fixed current densities and temperatures close to T_c. We pay special attention to the possible existence of a stationary regime. If the contacts are superconducting, truly stationary or normal regimes do not exist, but can be approached as a limit. In the case of weak superconducting contacts, a rich phase diagram is found, with several periodic regimes that involve two phase slip centers. There may be a time lag between the phase slips at each of these centers. There is a small parameter region in which this time lag is continuously tuned by the parameters. For some of these regimes, the density of Cooper pairs does not have mirror symmetry. If the contacts are normal, the stationary regime is possible. Analysis according to the Kramer–Watts-Tobin formalism leads to qualitatively the same results as the time-dependent Ginzburg-Landau model.

DOI: 10.1103/PhysRevB.92.064513 PACS number(s): 74.25.Dw, 74.20.De, 74.25.Sv

I. INTRODUCTION

When current is driven along a superconducting wire, it can either flow as normal current, as supercurrent, or as a combination of both. The various patterns that may be obtained in space and time were reviewed long ago [1,2], and a new approach [3], still within the phenomenological framework in which the superconducting condensate is described by an order parameter, has been raised in recent years. The results obtained for 1D wires have been extended to the case of stripes [4–7].

One of the possible patterns is periodic in time, and a salient feature of the periodic regime is the appearance of phase slips that occur when the superconducting order parameter vanishes at some point. Phase slips repeatedly occur at definite positions, called phase slip centers (PSC). While early studies (e.g., Refs. [1,2] and references therein) were mainly interested in wires of effectively infinite length, so that they extended over many PSC and were insensitive to the boundary conditions, Ref. [3] focuses on a parameter region in which there are just a few PSC, if any, since this is the region that most neatly exhibits the qualitative features of the current pattern.

For experimentally reasonable temperatures (not unfeasibly close to the critical temperature), the wires studied in Ref. [3] have to be short. On the other hand, wires that are too short cannot be analyzed as in Ref. [3] by means of the time-dependent Ginzburg-Landau model (TDGL) or its extensions. One of the most realistic of these extensions, the Kramer–Watts-Tobin (KWT) model [8–10], is justified provided that there is local equilibrium, and hence the requirements $D\tau_{\rm in} \ll \xi^2(T)$ and $D\tau_{\rm in} \ll L^2$, where D is the diffusion constant, $\tau_{\rm in}$ is the inelastic collision time, $\xi(T)$ is the coherence length, and, following Ref. [3], we denote by L half the length of the wire. As a general trend, $\tau_{\rm in}$ decreases with temperature [11]; for Al $\tau_{\rm in} \sim 5\times10^{-8}$ sec and the shortest lengths that can be dealt by means of KWT are larger than 10 μm, whereas for Pb or Nb $\tau_{\rm in} \sim 2\times10^{-11}$ sec, leading to lengths of the order of 10^{-1} μm. Furthermore, KWT is not reliable in the analysis of features that last less than $\tau_{\rm in}$. Shorter wires [12–14] can be analyzed by means of the Usadel [15] or similar equations.

For $\tau_{\rm in} \to 0$, KWT reduces to TDGL. For realistic situations TDGL is not quantitatively correct below T_c, but Ref. [3] states that their essential results, obtained for $\tau_{\rm in} = 0$, remain valid for finite $\tau_{\rm in}$. Therefore, since TDGL permits faster evaluations, since its results can be scaled to arbitrary length, and since we are mainly interested in qualitative results, we will conduct most of our study within the TDGL framework, and then use KWT to recalculate the results that seem to be the most fragile.

Figure 1 shows the phase diagram for the flow patterns, for small currents and for temperatures close to T_c, that is obtained with the method and boundary conditions used in Ref. [3], but for realistic material parameters. Below the pertinent curve the sample is in the normal state (N) and all the current is normal, whereas above the curve there is a stationary regime (S), in which normal current and supercurrent are both present; both are functions of position, but none of them depends on time. The stationary regime was previously found in Ref. [16]. In several cases [10,12,13,17] a stationary regime has been postulated by excluding time derivatives in the evolution equations (thus leaving open the question of stability). The third possibility found in Ref. [3] is the periodic regime, in which the normal current and the supercurrent are periodic functions of time, but for realistic material parameters the periodic regime is strongly disfavored in comparison to the stationary state [18].

The question arises of why, whereas Fig. 1 or Ref. [16] suggest that the most frequently encountered superconducting phase is stationary, emphasis is usually [1,2,10,19,20] placed on periodic regimes. One reason for this disparity is the small effective length of the wires considered in references such as [3,16], or [18]. We argue that the other reason is that these studies assume that the order parameter vanishes at the boundaries.

As we will spell out in Sec. II C, the order parameter does vanish at the boundaries if the "banks" from which the current is fed are made of magnetic materials. In the present study we will compare this situation with other possibilities: the banks

*jorge.berger@braude.ac.il

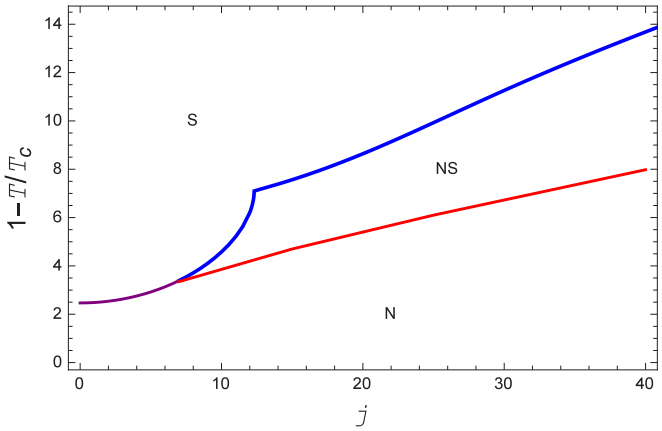

FIG. 1. (Color online) Phase diagram for the current-flow regimes in the current density–temperature plane, if the order parameter vanishes at the extremes of the wire and $u = 5.79$. "S" denotes stationary regime, "N" denotes exclusively normal current, and "NS" denotes a region where both regimes are possible and stable, so that the actual regime depends on history. The blue line is the stability limit when either the current or the temperature decreases (i.e., the normal state is stable up to this line), the red line is the stability limit when they increase (i.e., the stationary regime is stable down to this line), and the purple line is the stability limit in both directions. The unit of current density, j_0, is defined in Eq. (1). Following Ref. [3], we have taken a wire of length $2\xi(0)$; for length $2L$, the values of $1 - T/T_c$ in this diagram have to be multiplied by $[L/\xi(0)]^{-2}$ and those of j by $[L/\xi(0)]^{-3}$.

will be either superconducting, or normal metals that obey the de Gennes boundary condition. We will also consider the limiting case of very weak superconductors, and examine in what sense the stationary regime is approached.

II. ANALYSIS BASED ON TDGL

Following Refs. [3] and [16], we use a minimal model. The wire will be perfectly 1D and uniform, we will assume electroneutrality, and superconductivity will be described by the time-dependent Ginzburg-Landau model. We choose a gauge with no vector potential, write $\Gamma = 1 - T/T_c$, and denote by φ the electrochemical potential. The unit of length will be denoted by x_0, by t_0 the unit of time, by φ_0 the unit of voltage, and by j_0 the unit of the current density. As in Ref. [18], we take

$$x_0 = \xi(0), \quad t_0 = \frac{\pi\hbar}{8k_BT_c}, \quad \varphi_0 = \frac{4k_BT_c}{\pi e}, \quad j_0 = \frac{4\sigma k_BT_c}{\pi e\xi(0)}. \tag{1}$$

Here $\xi(0)$ is the coherence length at $T = 0$, k_B is Boltzmann's constant, e is the electron charge, and σ is the normal conductivity.

With this notation, the TDGL equation and Ohm's law read

$$\psi_t + i\varphi\psi = \psi_{xx} + \Gamma\psi - |\psi|^2\psi \tag{2}$$

and

$$\varphi_x = u\,\mathrm{Im}(\psi_x\psi^*) - j. \tag{3}$$

Here ψ is the order parameter, with normalization imposed by Eq. (2), the subscripts denote partial differentiation with respect to the time t and the arc length x along the wire, and u is the ratio between the relaxation times of ψ and j [21].

Our model neglects Joule heating and thermal fluctuations. Joule heating can be neglected provided that the current density is sufficiently small and/or the wire is sufficiently thin and in good thermal contact with a heat bath. Thermal fluctuations are expected to be important near stability limits.

The wire is assumed to extend along $-L \leqslant x \leqslant L$. Equations (2) and (3) are invariant under the transformation $x \to Lx, t \to L^2t, \psi \to L^{-1}\psi, \varphi \to L^{-2}\varphi, \Gamma \to L^{-2}\Gamma$, and $j \to L^{-3}j$, since each of the terms in Eqs. (2) and (3) is multiplied by L^{-3}. Therefore, if also the boundary conditions are invariant under this transformation, we can limit our study to a single value of L, and the solutions for any other value are obtained by scaling. We note that $L/\xi(T)$ is invariant under this scaling.

A. Banks of same material as the wire

The most common experimental situation is that the banks and the wire are carved from the same layer. The banks are located at the extremes of the wire, $x = \pm L$, and are much wider than the wire, so that the current density in them is negligible. The banks can therefore be treated as being in equilibrium, and we obtain from Eq. (2) that $|\psi(\pm L)| = \Gamma^{1/2}$. The phase of the order parameter has to obey the Josephson relation and we therefore require the boundary conditions

$$\psi(\pm L,t) = \Gamma^{1/2}\exp\left[-i\int_0^t \varphi(\pm L,t')dt'\right]. \tag{4}$$

The electrochemical potential φ is obtained from Eq. (3), in which we will set $u = 5.79$, as appropriate for a dirty superconducting material without magnetic impurities [21,22].

For given values of j and Γ, Eqs. (2)–(4) were solved numerically; numerical details are provided in the Appendix. The evolution of the order parameter ψ and the potential φ was followed until a stationary or periodic regime was attained. j and/or Γ were gradually varied, and for each set (j,Γ) the initial values of ψ were taken from its final values for a nearby (j,Γ) (except in the case of the first set, for which a reasonable function ψ had to be deduced or guessed). When evolution leads to a regime that is qualitatively different than the previous one, it means that a stability boundary has been crossed.

Figure 2 shows the phase diagram that we encounter for boundary condition (4). In contrast to Fig. 1, the possible regimes are either purely superconducting (SC), i.e., no normal current flows along the wire, or periodic. The periodic regime that we encounter has a single PSC, located at the middle of the wire, and we denote this regime by P1.

It is clear that a strictly normal regime is incompatible with the condition (4), since the order parameter cannot vanish close to $x = \pm L$. Also the stationary regime is implausible: normal currents would imply dissipation, so that $\varphi(L) < \varphi(-L)$. In this case condition (4) implies winding that increases with time, and can only be released if the order parameter vanishes at some point, so that phase slips are expected.

It should be mentioned that although in the periodic regime there is a voltage drop along the wire, this problem is not equivalent to the case of fixed applied voltage studied in,

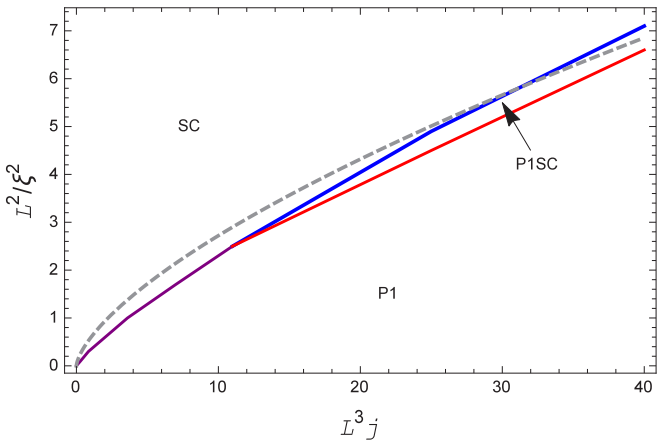

FIG. 2. (Color online) Phase diagram if the contacts to the wire are made of the same superconducting material as the wire. L is half the length of the wire, the units of length and current density are defined in Eq. (1), and the y axis is $L^2/\xi^2(T) = \{L^2/[\xi^2(0)T_c]\}(T_c - T)$. "SC" stands for exclusively superconducting current, "P1" stands for periodic regime with one phase slip center at the middle of the wire, and "P1SC" denotes a region where both regimes are possible. The dashed gray curve corresponds to the critical current density $j_c = 2u(\Gamma/3)^{3/2}$, that would be obtained in a very long wire in which the boundaries become irrelevant. The meaning of the other line colors is the same as in Fig. 1.

e.g., Refs. [23] and [24]. In the present case $\varphi(-L) - \varphi(L)$ is periodic, rather than constant in time.

If there is no normal current and if the order parameter has uniform size, then Eqs. (2) and (3) imply that the maximum current density is $j_c = 2u(\Gamma/3)^{3/2}$. j_c is called the "critical current density," and it is usually stated that the wire is in the normal state for $j > j_c$. In Fig. 2 we see that the constraint $|\psi(\pm L)| = \Gamma^{1/2}$ favors the superconducting regime for small currents, but inhibits it for large currents.

Since the wire cannot be strictly normal, we investigate in what sense the normal regime is approached when j rises above j_c. Figure 3 shows the size of the order parameter $|\psi(x,t)|$ for two current densities above j_c. We see that the periodic regime persists, but phase slips become more frequent for larger currents, and therefore the order parameter has less time to recover and remains small. In the studied region ($L^3 j \leqslant 40$), increase of $L^3 j$ does not lead to additional PSC along the wire.

B. Banks of a superconducting material that is weaker than that of the wire

We consider now the case that the wire and the banks are made of different superconducting materials, so that $|\psi(\pm L,t)| \neq \Gamma^{1/2}$. We write $|\psi(\pm L,t)| = r\Gamma^{1/2}$ and replace the boundary condition (4) with

$$\psi(\pm L,t) = r\Gamma^{1/2} \exp\left[-i \int_0^t \varphi(\pm L,t')dt'\right]. \qquad (5)$$

We will especially be interested in the case that r is significantly less than 1. A related study with similar assumptions was carried out in Ref. [25].

In this case we find a surprisingly rich phase diagram. Figure 4 shows the phase diagram obtained for $r = 0.05$. In addition to the regimes SC and P1 already found for $r = 1$, we find additional regimes that mediate between them. These regimes are periodic with two PSC at symmetric positions with respect to the middle of the wire. Sometimes we found that both phase slips occur simultaneously and we denote this regime by P2. We also found cases in which the two phase

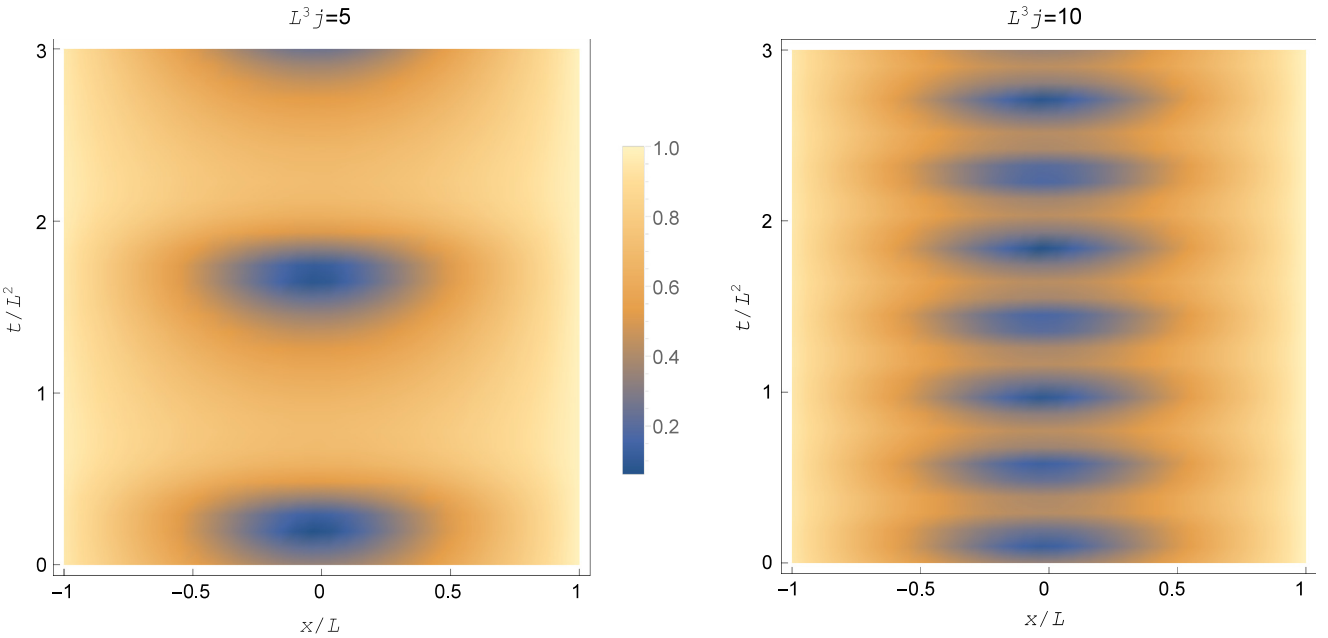

FIG. 3. (Color online) Density plot of the absolute value of the order parameter, $|\psi(x,t)|$, for current densities above the "critical current density," j_c (the largest uniform supercurrent density that can be carried by an infinitely long wire). In these plots we took $\xi(T) = L$, so that $j_c = 2.23 j_0 \xi^3(0)/L^3$. The banks are made of the same material as the wire. According to Fig. 2, both plots correspond to the periodic regime P1. The color bar is common to both plots and shows the value of $L|\psi|$.

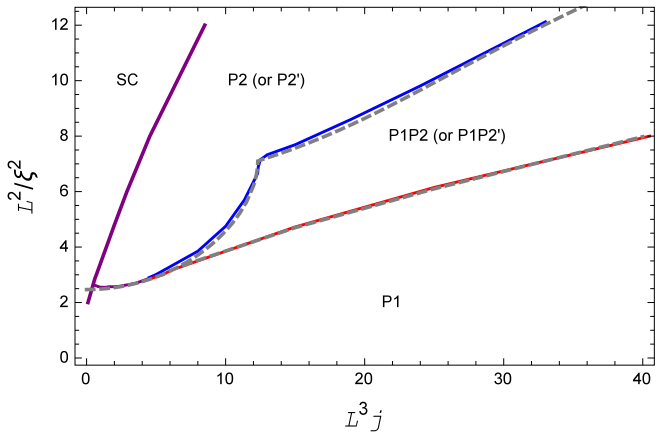

FIG. 4. (Color online) Phase diagram if the order parameter at the contacts is smaller by a factor 0.05 than what it would be if the banks and the wire were of the same material. "P2" (or "P2′") stands for periodic regime with two phase slip centers, "SC" and "P1" have the same meaning as in Fig. 2, and "P1P2" (or "P1P2′") denotes a region where one or two PSC are possible. The dashed gray curves are the stability lines for $r = 0$, presented in Fig. 1.

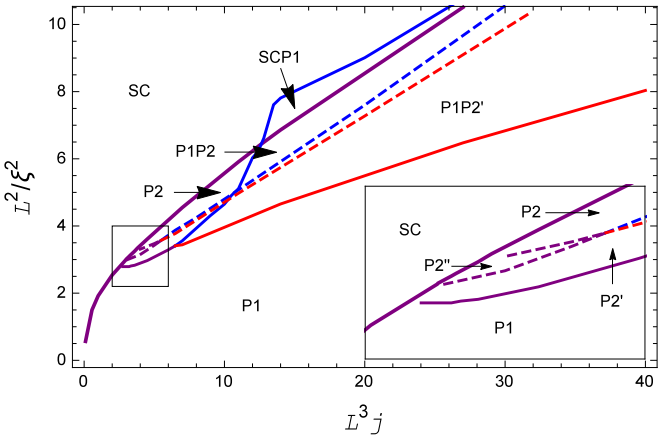

FIG. 5. (Color online) Phase diagram for $r = 0.2$. The colors of the stability boundaries are as in Fig. 1, and "P2", "SC", "P1", and "P1P2" have the same meaning as in Fig. 4. Likewise, SCP1 and P1P2′ are regions where two regimes are possible. The stability boundaries that involve two regimes that both have two PSC are depicted by dashed lines. The framed region $2 \leqslant L^3 j \leqslant 6$ and $2.2 \leqslant L^2/\xi^2(T) \leqslant 4$ is shown in an enlarged scale in the inset. Between the red and the blue dashed lines, P2, P2′, and P1 are possible.

slips are separated in time by half a period, and denote this regime by P2′. The stabilization time required to pass between the situations P2 and P2′ is very long [several times $10^3\, t_0$ for $L = \xi(0)$]. We did not investigate the stability boundaries between P2 and P2′ for $r = 0.05$, but this will be done for $r = 0.2$. The upper stability boundary of P1 almost coincides with the upper stability boundary of the normal regime in the case $\psi(\pm L) = 0$, and the lower boundary of P2 almost coincides with the lower boundary of the stationary regime.

It should be born in mind that, for given materials, r is a function of temperature. Therefore, the phase diagrams for fixed r should not be directly interpreted as phase diagrams in the current density–temperature plane. As r increases, the region occupied by the purely superconducting regime increases, and the topology of the phase diagram can change. Figure 5 shows the phase diagram for $r = 0.2$. We note that in this case there is a region where SC and P1 are both possible and that the stability boundaries of P2 and P2′ have been investigated separately.

For $L^3 j \lesssim 5.5$, the transition between P2 and P2′ in Fig. 5 is continuous. In this range P2 and P2′ are mediated by a regime with two PSC, that we denote by P2″, in which the time lag changes gradually with decreasing $L/\xi(T)$ from zero to half a period. Figure 6 shows density plots of $|\psi(x,t)|$ for $L^3 j = 4$, for $L/\xi = 1.73$ (P2′ regime) and for $L/\xi = 1.8$ (P2″ regime).

Within the framework of TDGL or KWT, we are not aware of previous reports of situations in a uniform superconducting wire such that the order parameter obeys $|\psi(-L,t)| = |\psi(L,t)|$, but stabilizes in a regime in which $|\psi(-x,t)| \neq |\psi(x,t)|$. On the other hand, this symmetry breaking has been encountered using a Usadel analysis [14,17].

It is hard to judge numerically whether situations as the case $L/\xi = 1.8$ in Fig. 6 truly correspond to a distinct P2″ regime, or are rather encountered due to insufficient stabilization time. We believe they correspond to a distinct regime, because starting from different initial order parameters we obtain the same time lag between consecutive phase slips.

Since Figs. 4 and 5 show no hysteresis in the transition between SC and P2, we expect a continuous transition. At first sight this seems impossible, since in P2 the order parameter approaches zero at the phase slips, whereas in SC it does not, so that an infinitesimal change in the current density can lead to finite differences in the order parameters when a phase slip occurs. The paradox is resolved by Fig. 7, that shows that the time between consecutive phase slips diverges when the SC regime is approached, so that P2 approaches SC almost everywhere in the xt plane. The inset in the figure shows that the same effect occurs when the P2 $\rightarrow$ SC transition is due to increase of r.

An experimentally accessible quantity is the dc component of the voltage drop along the wire. Figure 8 shows this quantity for the same parameters as in Fig. 7, which involve a hysteresis region.

For the parameters chosen in Figs. 7 and 8 the position of the PSC in the P2 regime are almost independent of j. Also in the P2′ regime these positions are almost fixed in most of the stability range, but in the case of a continuous transition to P1, very near the transition, the PSC migrate to the center of the wire, and thus the P1 regime is obtained and the period is halved. Also in Ref. [26], which considered banks of the same material as the wire, and assumed $u = 0.5$ and no normal current at the banks, bifurcations with period jumps by a factor of two and divergence of the period at a critical current were found.

We are now in a position to discuss in what sense the P2 regime approaches the stationary regime in the limit $r \rightarrow 0$. We first note from Fig. 9 that in this limit the PSC approach the extremes $x = \pm L$ of the wire, and that at these PSC the order parameter $\psi_{\rm PSC}$ is bound to the size $|\psi_{\rm PSC}| \leqslant 2r\xi^2(0)/L\xi(T)$. Therefore $\psi(\pm L) \rightarrow 0$ for $r \rightarrow 0$, as expected, and there are no phase slips in the interior of the wire.

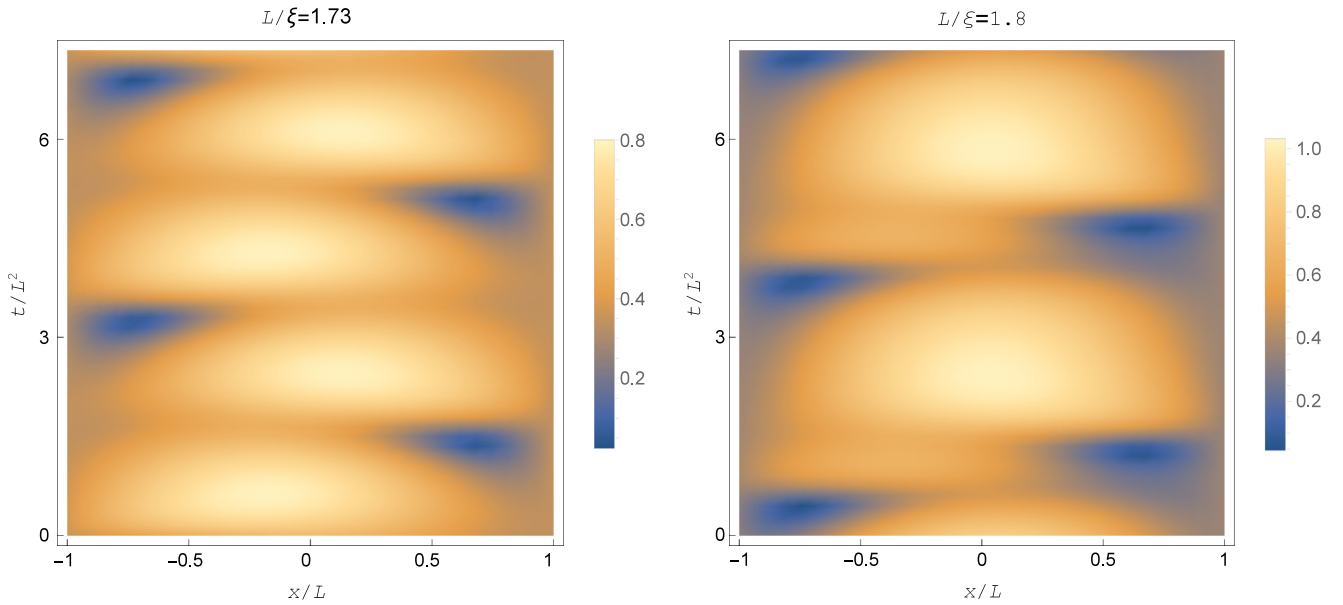

FIG. 6. (Color online) Density plots of $|\psi(x,t)|$ for $r = 0.2$ and $L^3 j = 4$. The case $L/\xi = 1.73$ is in the P2′ regime and the case $L/\xi = 1.8$ is in the P2″ regime. The color bars show the value of $L|\psi|$.

Next, we recall that a peculiar measurable property of the stationary regime is that the potential felt by Cooper pairs, $-\varphi_0 t_0 \partial \arg\psi/\partial t$ (that can be probed by means of SIS junctions, as in Ref. [19]) is independent of position. Quite generally, we can conclude that if $x = x_1$ and $x = x_2$ are two points of the wire such that $\psi(x_1,t)$ and $\psi(x_2,t)$ are periodic and there is no PSC in the segment $x_1 \leqslant x \leqslant x_2$, then the time averages of $\partial \arg\psi/\partial t$ at $x = x_1$ and at $x = x_2$ have to be equal. Otherwise, $|\arg\psi(x_1) - \arg\psi(x_2)|$ would endlessly increase, the order parameter would become increasingly wound up, and this would force phase slips in the segment $x_1 \leqslant x \leqslant x_2$. Summing up, we conclude that in the P2 regime the time average of $\partial \arg\psi/\partial t$ is uniform in the segment between the PSC, and in the limit $r \to 0$ this property applies to the entire wire.

In contrast to the stationary regime, in the case of P2 the potential felt by Cooper pairs is not independent of position for arbitrary times in the segment between the PSC. Figure 10 shows the potentials felt by Cooper pairs and by normal electrons between two given points, as functions of time, during a period. The normal potential peaks shortly after the phase slips.

C. Banks of a normal metal

In the spirit of a minimal model description, we adopt the de Gennes boundary condition [27,28]

$$\psi_x(\pm L) = \mp\psi(\pm L)/b, \tag{6}$$

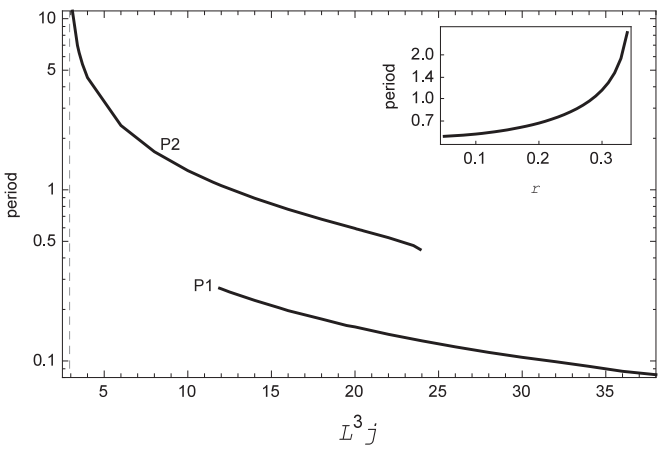

FIG. 7. Duration of a period, in units of $\pi\hbar L^2/8k_B T_c\xi^2(0)$, as a function of the current density for the P2 regime (upper curve) and for the P1 regime (lower curve), for $L^2\Gamma = 6$ and $r = 0.05$. The curves end where these regimes stop to exist. The gray dashed line indicates the transition between P2 and SC. The y axis is logarithmic. Inset: Period in the P2 regime as a function of r, for $L^2\Gamma = 7$ and $L^3 j = 24$; at $r \approx 0.34$ there is a transition between P2 and SC.

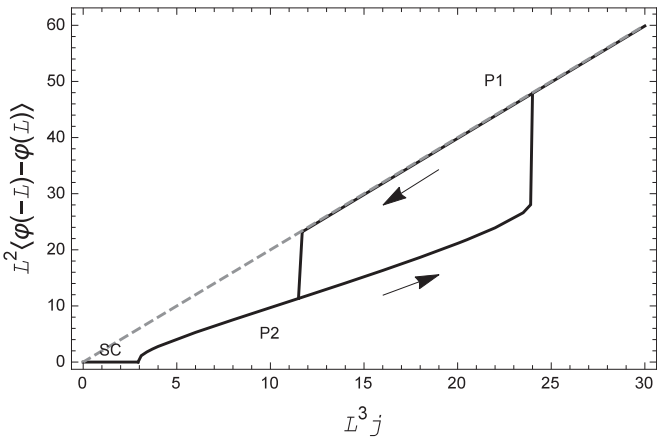

FIG. 8. Time average of the voltage drop along the wire, as a function of the current density, for $L^2\Gamma = 6$ and $r = 0.05$. The arrows indicate the direction in which the current is varied. The gray dashed line shows the voltage that would be obtained if the wire were in the normal state.

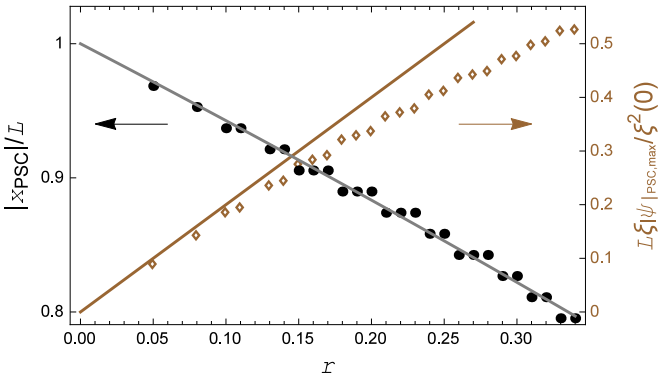

FIG. 9. (Color online) The black dots (left y axis) show the distance between the phase slip centers and the middle of the wire in the P2 regime as a function of r, for $L^2\Gamma = 7$ and $L^3 j = 24$. The brown squares (right y axis) show the maximum size of the order parameter at these phase slip centers. The gray line is a guide for the eye and the brown straight line has slope 2. The staircase appearance is due to the finite discretization of position.

where b is a length that represents how far Cooper pairs can survive inside the normal metal. The material parameter b can assume a wide range of values; the limit $b \to \infty$ corresponds to an insulator and $b \to 0$ corresponds to a magnetic material. If the bank is made of a dirty metal or semimetal with no magnetic impurities, then $b = (\sigma/\sigma_N)(\hbar D_N/2\pi k_B T)^{1/2}$, where σ_N and D_N are the electric conductivity and the diffusion constant in the bank. Condition (6) can be justified microscopically for static situations, and we may expect that it is still qualitatively correct for small current densities. Since the supercurrent density is proportional to $\mathrm{Im}(\psi_x \psi^*)$, condition (6) implies that there is no supercurrent at the contacts; therefore this condition may also be an appropriate description of the case in which quasiparticles are injected and withdrawn from the wire by means of NIS junctions. Also when the Usadel equations are used, experiments suggest that the pairing angle obeys a boundary condition analogous to Eq. (6) [12,13]. The scaling with length introduced above has to be supplemented with $b \to Lb$.

Within a numerical scheme in which position along the wire is replaced by a computational grid and $\psi_x(\pm L)$ are approximated by finite differences, condition (6) becomes $\psi(\pm L) = b\psi(\pm L \mp \Delta x)/(b + \Delta x)$, where Δx is the length of a segment in the grid. Unlike the previous sections, the order parameter is not continuous at the boundaries, and the relevant values in Eq. (6) are those inside the wire. Since there is no equilibrium in the wire, the rate of change of the phases at the boundaries is not dictated by the potential, and it is therefore possible to have $\varphi(-L) \neq \varphi(L)$ without phase slips, so that the stationary regime is not ruled out.

The stability boundary of the normal regime can be found as in Ref. [3], since the evolution equations and the boundary conditions are PT-symmetric [3], and all the theorems shown in Ref. [29] apply here as well. The normal regime is unstable if Eqs. (2), (3), and (6) have a solution of the form $\psi(x,t) = f(x)e^{(\Gamma-\gamma)t}$ with $\mathrm{Re}(\gamma) < \Gamma$. At the bifurcation from N the nonlinear terms in Eqs. (2) are (3) negligible, and we are left with the spectral problem

$$f_{xx} + ixjf = -\gamma f, \quad f_x(\pm L) = \mp f(\pm L)/b, \tag{7}$$

where γ is the eigenvalue with the smallest real part. The real part of this eigenvalue is the largest value of Γ for which N can be stable.

Figure 11 is the phase diagram that we found for $b = 0.2L$. In comparison with the case $b = 0$, we see that the boundaries move to higher temperatures and the Hopf singularity moves to a lower current density, but the topology is the same as in the case $b = 0$, and the stationary regime still exists. For the purpose of comparison with KWT, that will be studied in the following section, the length of the wire has been fixed.

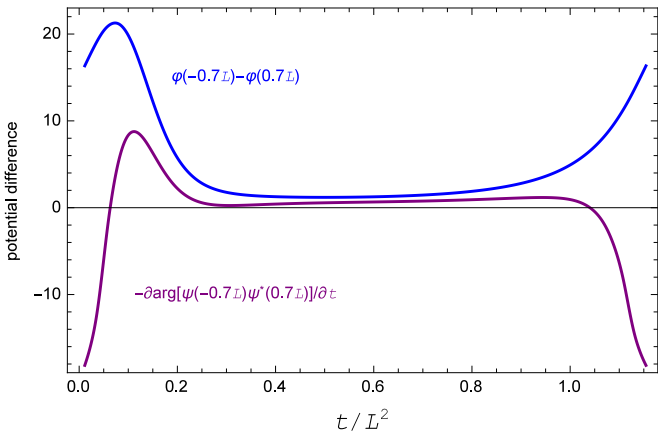

FIG. 10. (Color online) Potential differences felt by normal electrons and by Cooper pairs between the points $-0.7L$ and $0.7L$, in units of $4k_B T_c \xi^2(0)/\pi e L^2$, for a situation in the P2 regime. The graph extends over one period, and the origin of time was set when a pair of phase slips occurs. The parameters used were $L^2\Gamma = 7$, $L^3 j = 24$, and $r = 0.3$. For these parameters the PSC are at $\pm 0.83L$.

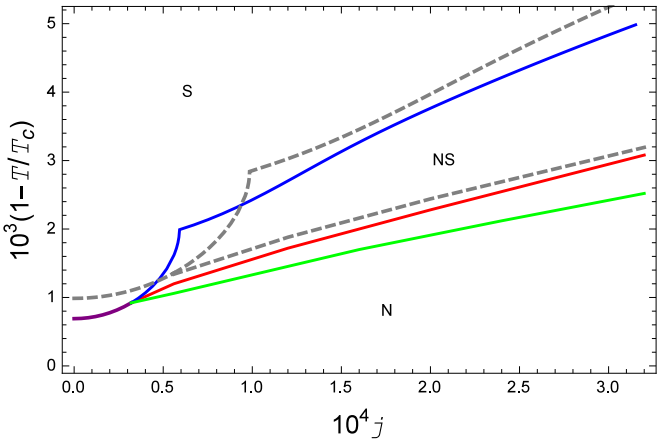

FIG. 11. (Color online) Phase diagram in the case of normal banks with de Gennes parameter $b = 0.2L$, for a wire of length $2L = 100\xi(0)$. S stands for the stationary regime and N for the normal regime. The blue, the red, and the purple lines have the same meaning as in Fig. 1. The dashed gray curves are the stability lines for $b = 0$, presented in Fig. 1. The green line is the stability limit of the stationary state that is obtained from KWT (Sec. III) with $u\tau_{\mathrm{in}}^2 = 10^4 t_0^2$. The stability limit of the normal regime is obtained from the eigenvalue with the smallest real part in Eq. (7).

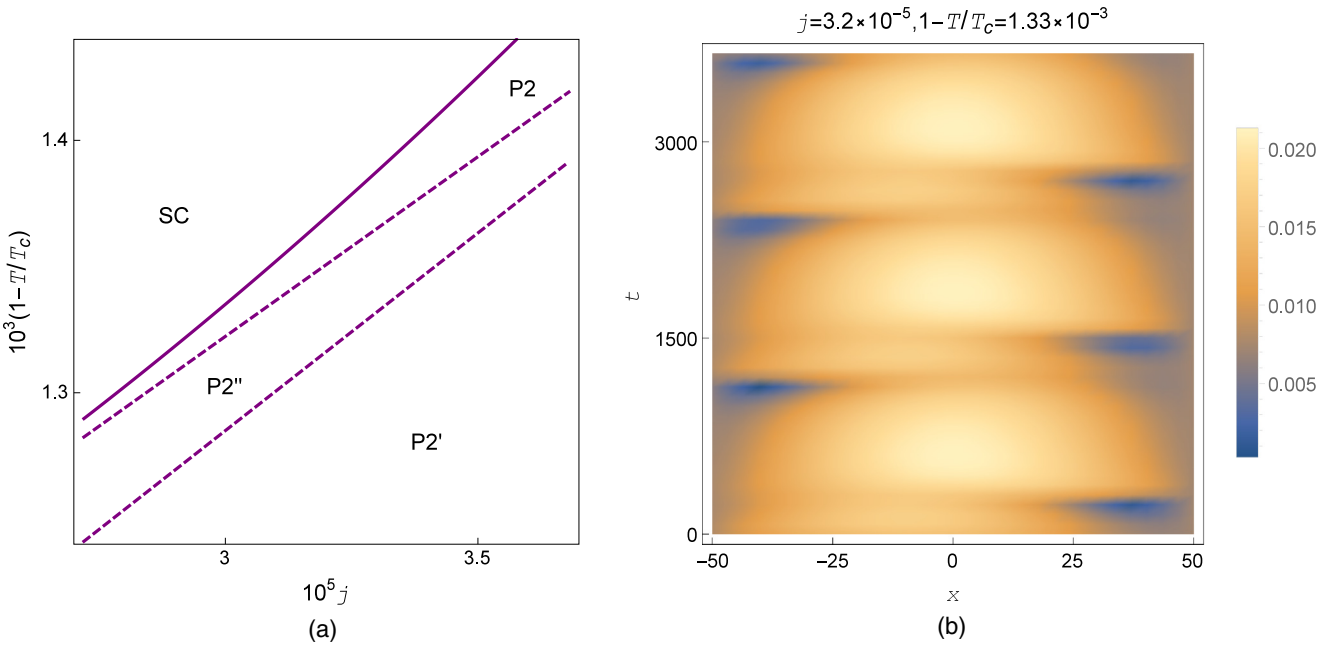

FIG. 12. (Color online) Results obtained using the KWT model for $u\tau_{\rm in}^2 = 10^4 t_0^2$, $L = 50\xi(0)$, and $r = 0.2$. (a) Phase diagram in a small region, that includes an area where the P2″ phase is found. (b) Density plot of $|\psi(x,t)|$ for $j = 3.2\times10^{-5} j_0$ and $1 - T/T_c = 1.33\times10^{-3}$.

III. ANALYSIS BASED ON KWT

We now replace Eq. (2) with [8]

$$\left(1+u\tau_{\rm in}^2|\psi|^2\right)^{-1/2}\left(\partial_t + i\varphi + \frac{u\tau_{\rm in}^2}{2}\frac{\partial|\psi|^2}{\partial t}\right)\psi = \psi_{xx} + (\Gamma - |\psi|^2)\psi. \quad (8)$$

Multiplying Eq. (8) by ψ^* and taking the real part we obtain, after some algebra,

$$(1/2)\,\partial|\psi|^2/\partial t = \left(1+u\tau_{\rm in}^2|\psi|^2\right)^{-1/2}[{\rm Re}(\psi^*\psi_{xx}) + (\Gamma - |\psi|^2)|\psi|^2], \quad (9)$$

and substituting back, Eq. (8) takes a form that is appropriate for Euler iterations:

$$\psi_t = \left(1+u\tau_{\rm in}^2|\psi|^2\right)^{1/2}\psi_{xx} - i\varphi\psi + \left(1+u\tau_{\rm in}^2|\psi|^2\right)^{-1/2}[\Gamma - |\psi|^2 - u\tau_{\rm in}^2{\rm Re}(\psi^*\psi_{xx})]\psi. \quad (10)$$

Unlike Eq. (2), Eq. (8) is not invariant under the scaling transformations with length, and therefore we have to specify the length of the wire. Here we take $2L = 100\xi(0)$ and $u\tau_{\rm in}^2 = 10^4 t_0^2$, of the order of magnitude in the cases of Pb or Nb. The time steps used in our iterations were of the order of $10^{-2}t_0$. We limited this section to the study of two situations: the P2″ region described in the inset of Fig. 5, and the case of a normal conductor at the boundaries.

Figure 12(a) focuses on a parameter range that contains the P2″ phase, for banks that are weaker superconductors than the wire, and Fig. 12(b) depicts the behavior of the order parameter in this region. In the case of Fig. 12(b), evolution was followed during $\sim 5\times10^6 t_0$ and the time lag between phase slips at different sides of the wire remained unchanged within four significant figures.

The phase diagram for normal banks that we obtain using KWT has been added to Fig. 11. Since for $\psi \to 0$ KWT reduces to TDGL, the stability limit of the normal regime is the same as for TDGL, and this also holds for the stability limit of the stationary state if the transition is continuous.

We now check the applicability of KWT to the example studied in this section. Noting that $\xi^2(0) = Dt_0$, the conditions $D\tau_{\rm in} \ll \xi^2(T)$ and $D\tau_{\rm in} \ll L^2$, required for accuracy of KWT, are equivalent to $\tau_{\rm in} \ll t_0(1-T/T_c)^{-1}$ and $\tau_{\rm in} \ll t_0 L^2/\xi^2(0)$. The conditions for marginal applicability of KWT are $\tau_{\rm in} \lesssim t_0(1-T/T_c)^{-1}$ and $\tau_{\rm in} \lesssim t_0 L^2/\xi^2(0)$. Since for Pb or Nb the ratio $\tau_{\rm in}/t_0$ is smaller than 10^2, the first condition is fulfilled for $T > 0.99T_c$ and the second condition is fulfilled for the length we chose. We also note that the duration of a period in Fig. 12 is of the order of $10^3 t_0$, sufficiently larger than $\tau_{\rm in}$ to enable equilibration, so that the use of KWT is justified in the analysis of these oscillations. It is worth mentioning that in Fig. 12 $u\tau_{\rm in}^2|\psi|^2$ reaches values of the order of 5, beyond the limit of applicability of TDGL and of scaling with length.

Figures 11 and 12 support the claim [3] that KWT does not lead to any surprises within the region we have studied, so that TDGL provides a valid qualitative description of the patterns of current flow in a 1D wire.

IV. CONCLUSIONS

We have studied the patterns of current flow along a one-dimensional superconducting wire, for various boundary conditions, for current densities smaller than $160\sigma k_B T_c \xi^2(0)/\pi e L^3$ and temperatures in the range $T_c[1 - 12\xi^2(0)/L^2] \leqslant T < T_c$. Most of our results were obtained using TDGL. The most relevant obtained features were revised using the Kramer–Watts-Tobin model, and were found to be qualitatively valid. In the present analysis we have not taken fluctuations into account; this can be an important omission in reduced cross sectional wires near T_c.

A stationary regime, in which all observable fields are independent of time, was previously found under the assumption that the order parameter vanishes at the extremes of a superconducting wire. Our results clarify to what extent and in what sense the stationary regime can exist when the order parameter is not forced to vanish at these boundaries. If the contacts are normal and the de Gennes boundary condition is assumed, the stationary regime still exists and the phase diagram is qualitatively unchanged, even if the de Gennes length is not negligible in comparison to the length of the wire. The stationary regime might find applications in cases in which oscillations would induce disturbances (e.g., back action from a SQUID).

If the contacts are superconducting, but weaker than the wire, the phase diagram changes qualitatively, and several new features arise. The role of the normal regime in Refs. [3] and [16] is inherited by a periodic regime with one phase slip center, and the order parameter converges nonuniformly to zero as the current density increases. Part of the region in which Refs. [3] and [16] found the stationary regime becomes now fully superconducting (there is no normal current). The fully superconducting regime and the periodic regime with one PSC are mediated by one or several periodic regimes with two PSC. In the limit that the contacts are made of very poor superconductors, the regime with two PSC becomes similar to the stationary state, since the PSC approach the extremes of the wire, and the time average of the potential felt by Cooper pairs is uniform between them.

In the regime with two PSC, the two phase slips may be simultaneous, but there may also be a time lag between them. When a time lag is present, the solution of the dynamic equations breaks the symmetry of the equations, and $|\psi(-x,t)| \neq |\psi(x,t)|$.

ACKNOWLEDGMENTS

This research was supported by the Israel Science Foundation, Grant No. 249/10. Numeric evaluations were performed using computer facilities of the Technion–Israel Institute of Technology. The author is indebted to John Kirtley, Jacob Rubinstein, Raymond Simmonds, and Eli Zeldov for their answers to his enquiries.

APPENDIX: NUMERICAL SOLUTION OF THE DYNAMIC EQUATIONS

The wire was discretized into a grid of 2^7 vertices and time into steps of $3\times10^{-5}t_0L^2/\xi^2(0)$. We started with an arbitrary function for the order parameter $\psi(x)$; if available, we took a function obtained from evolution with similar parameters, and otherwise we usually took $\psi \equiv r\Gamma^{1/2}$.

Derivatives with respect to x were obtained as follows: a fast Fourier transformation was performed on $\psi(x)$, and the Fourier transformed function was multiplied by $(ik)^p$, where k is the reciprocal variable of x and p is the order of the desired derivative. We then transformed back to x space and obtained $\partial^p\psi/\partial x^p$.

The problem with this method is that it requires that ψ be periodic with period $2L$, and in particular that $\psi(-L) = \psi(L)$. Since this is not necessarily the case, we start by evaluating the derivative of $\psi'(x) = \psi(x) - [\psi(L) - \psi(-L)]x/(2L)$, which does obey $\psi'(-L) = \psi'(L)$, and subsequently add the derivative of $[\psi(L) - \psi(-L)]x/(2L)$. We are still left with the problem that the periodic extension of ψ' is not smooth at $\pm L$ and we cannot evaluate its derivatives at the boundaries. However, ψ_{xx} is not required at the boundaries, and $\psi_x(\pm L)$ enters the problem after multiplication by the length $L/2^6$ of a segment, so that $\psi_x(\pm L)$ can be evaluated as a finite difference.

The additional stages of the solution of Eqs. (2)–(4) (or similar) pose no numerical difficulty: $\varphi(x)$ can be obtained by trapezoidal integration of Eq. (3) and the evolution of ψ can be followed by Euler iteration. Likewise, the phases of $\psi(\pm L)$ can be updated by subtraction of the product of the time step times $\varphi(\pm L)$.

[1] B. I. Ivlev and N. B. Kopnin, Adv. Phys. **33**, 47 (1984).
[2] R. Tidecks, *Current-Induced Nonequilibrium Phenomena in Quasi-One-Dimensional Superconductors* (Springer, Berlin, 1990).
[3] J. Rubinstein, P. Sternberg, and Q. Ma, Phys. Rev. Lett. **99**, 167003 (2007).
[4] A. G. Sivakov, A. M. Glukhov, A. N. Omelyanchouk, Y. Koval, P. Müller, and A. V. Ustinov, Phys. Rev. Lett. **91**, 267001 (2003).
[5] L. Peres-Hari, J. Rubinstein, and P. Sternberg, Physica D **261**, 31 (2013).
[6] G. Berdiyorov, K. Harrabi, F. Oktasendra, K. Gasmi, A. I. Mansour, J. P. Maneval, and F. M. Peeters, Phys. Rev. B **90**, 054506 (2014).
[7] Y. Almog, L. Berlyand, D. Golovaty, and I. Shafrir, J. Math. Phys. **56**, 071502 (2015).
[8] L. Kramer and R. J. Watts-Tobin, Phys. Rev. Lett. **40**, 1041 (1978).
[9] R. J. Watts-Tobin, Y. Krähenbühl, and L. Kramer, J. Low Temp. Phys. **42**, 459 (1981).
[10] L. Kramer and R. Rangel, J. Low Temp. Phys. **57**, 391 (1984).
[11] B. Kaplan, C. C. Chi, D. N. Langenberg, J. J. Chang, S. Jafarey, and D. J. Scalapino, Phys. Rev. B **14**, 4854 (1976).
[12] G. R. Boogaard, A. H. Verbruggen, W. Belzig, and T. M. Klapwijk, Phys. Rev. B **69**, 220503(R) (2004).
[13] N. Vercruyssen, T. G. A. Verhagen, M. G. Flokstra, J. P. Pekola, and T. M. Klapwijk, Phys. Rev. B **85**, 224503 (2012).
[14] M. Serbyn and M. A. Skvortsov, Phys. Rev. B **87**, 020501(R) (2013).
[15] K. D. Usadel, Phys. Rev. Lett. **25**, 507 (1970).
[16] L. Kramer and A. Baratoff, Phys. Rev. Lett. **38**, 518 (1977).
[17] D. Y. Vodolazov and F. M. Peeters, Phys. Rev. B **75**, 104515 (2007).
[18] S. Kallush and J. Berger, Phys. Rev. B **89**, 214509 (2014).
[19] G. J. Dolan and L. D. Jackel, Phys. Rev. Lett. **39**, 1628 (1977).
[20] A. M. Gulian and G. F. Zharkov, *Nonequilibrium Electrons and Phonons in Superconductors* (Kluwer, New York, 1999).

[21] N. B. Kopnin, *Theory of Nonequilibrium Superconductivity* (Clarendon Press, Oxford, 2001).
[22] A. Schmid, Phys. Kondens. Materie **5**, 302 (1966).
[23] D. Y. Vodolazov, F. M. Peeters, L. Piraux, S. Mátéfi-Tempfli, and S. Michotte, Phys. Rev. Lett. **91**, 157001 (2003).
[24] J. Kim, J. Rubinstein, and P. Sternsberg, Physica C **470**, 630 (2010).
[25] K. K. Likharev and L. A. Yakobson, Zh. Eksp. Teor. Fiz. **68**, 1150 (1975) [Sov. Phys. JETP **41**, 570 (1976)].
[26] V. V. Baranov, A. G. Balanov, and V. V. Kabanov, Phys. Rev. B **84**, 094527 (2011).
[27] P. G. de Gennes, *Superconductivity of Metals and Alloys* (Westview Press, Boulder, 1999); Rev. Mod. Phys. **36**, 225 (1964).
[28] G. Deutscher and P. G. de Gennes, in *Superconductivity*, Part 2, edited by R. D. Parks (Marcel Dekker, New York, 1969).
[29] J. Rubinstein, P. Sternberg, and K. Zumbrun, Arch. Rational Mech. Anal. **195**, 117 (2010).